

Micropipet Delivery–Substrate Collection Mode of Scanning Electrochemical Microscopy for the Imaging of Electrochemical Reactions and the Screening of Methanol Oxidation Electrocatalysts

Cheng-Lan Lin, Joaquín Rodríguez-López, and Allen J. Bard*

Department of Chemistry and Biochemistry, Center for Electrochemistry, University of Texas at Austin, Austin, TX 78712

The micropipet delivery–substrate collection (MD–SC) mode of scanning electrochemical microscopy (SECM) is demonstrated. This new mode is intended for the study and imaging of electrochemical as well as electrocatalytic reactions of neutral species that cannot be generated electrochemically. The spontaneous transfer of the analyte from an organic solvent across an interface between two immiscible electrolyte solutions (ITIES) and its diffusion into the aqueous solution served as the mechanism to deliver it to the substrate, where the corresponding electrochemical or electrocatalytic reaction is carried out. High-resolution SECM images of ferrocenemethanol (FcMeOH) oxidation, benzoquinone (BQ) reduction, and the formic acid oxidation reaction (FAOR) at a Pt microelectrode substrate were successfully acquired. Furthermore, this new mode was used for the screening of electrocatalyst arrays for the methanol oxidation reaction (MOR), with the optimization of an efficient candidate, Pt₈₀Ce₂₀. Digital simulations produced quantitative information about the expected current response at the substrate in the proposed MD–SC mode of SECM.

Scanning electrochemical microscopy (SECM) in the tip generation–substrate collection (TG–SC) mode has been used successfully in the identification of efficient electrocatalysts. The current methodology, however, suffers from its inherent inability to study compounds that cannot be generated at the SECM tip electrochemically. In this study, this difficulty was overcome by introducing a method of delivery that is based on the partition of the species of interest across an aqueous/organic interface suspended from a micropipet.

In previous studies, the use of the SECM has allowed the development of a high throughput methodology for the screening of new bimetallic electrocatalysts, e.g., for the oxygen reduction reaction (ORR)^{1–4} and the H₂ oxidation reaction.^{5–9} A number

of different SECM modes can be employed in such screening,¹⁰ but the TG–SC mode is often most convenient. For example, in ORR studies a gold ultramicroelectrode (UME) was used as the tip to generate oxygen and scanned at a close distance above an electrocatalyst array, which consisted of small bimetallic electrocatalyst spots with different compositions. The ORR current response of each electrocatalyst spot was then collected at the substrate and compared to its neighbors to determine the optimum composition.

For the screening of new electrocatalysts using the above-mentioned TG–SC mode of the SECM, a fundamental requirement is that the species of interest be constantly generated at an UME tip. This requirement sets limitations to its applications, especially for those species that cannot be generated electrochemically with ease in a solution of interest, such as formic acid (FA) in acidic solution or methanol (MeOH). Our motivation is, then, to provide a suitable modification of the TG–SC methodology to encompass the needs for these applications, for either electrocatalyst screening or electrochemical reaction imaging purposes. The key issue is to develop a new method for the delivery of these species to a substrate. Although some efficient hydrodynamic methods exist,¹¹ the use of a diffusive system for the electrocatalyst screening method described above would be highly desirable.

The use of a micropipet with immiscible electrolyte solutions (ITIES) along with the SECM has been demonstrated to be an efficient technique to elegantly study the ion or electron transfer across liquid/liquid interfaces.^{12–15} In such experiments, a potential difference is applied across a liquid/liquid (organic/

* To whom correspondence should be addressed. E-mail: ajbard@mail.utexas.edu.

- (1) Fernández, J. L.; Walsh, D. A.; Bard, A. J. *J. Am. Chem. Soc.* **2005**, *127*, 357.
- (2) Walsh, D. A.; Fernández, J. L.; Bard, A. J. *J. Electrochem. Soc.* **2006**, *153*, E99.

- (3) Lin, C.-L.; Sanchez-Sanchez, C. M.; Bard, A. J. *J. Electrochem. Solid-State Lett.* **2008**, *11*, B136.
- (4) Black, M.; Cooper, J.; McGinn, P. *Meas. Sci. Technol.* **2005**, *16*, 174.
- (5) Jayaraman, S.; Hillier, A. *J. Phys. Chem. B* **2003**, *107*, 5221.
- (6) Shah, B.; Hillier, A. *J. Electrochem. Soc.* **2000**, *147*, 3043.
- (7) Jayaraman, S.; Hillier, A. *J. Comb. Chem.* **2004**, *6*, 27.
- (8) Jayaraman, S.; Hillier, A. *Langmuir* **2001**, *17*, 7857.
- (9) Kucernak, A.; Chowdhury, P.; Wilde, C.; Kelsall, G.; Zhu, Y.; Williams, D. *Electrochim. Acta* **2000**, *45*, 4483–4491.
- (10) Bard, A. J.; Mirkin, M. V. *Scanning Electrochemical Microscopy*; Marcel Dekker: New York, 2001.
- (11) Macpherson, J. V.; Marcar, S.; Unwin, P. R. *Anal. Chem.* **1994**, *66*, 2175–2179.
- (12) Shao, Y.; Mirkin, M. V. *J. Phys. Chem. B* **1998**, *102*, 9915.
- (13) Solomon, T.; Bard, A. J. *Anal. Chem.* **1995**, *67*, 2787.
- (14) Walsh, D. A.; Fernández, J. L.; Mauzeroll, J.; Bard, A. J. *Anal. Chem.* **2005**, *77*, 5182.

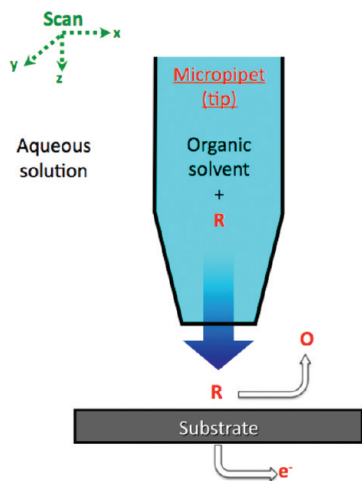


Figure 1. Representative operation scheme of the micropipet delivery–substrate collection mode of the SECM.

aqueous) interface. This potential difference serves as the driving force to pull ions from one phase into the other. The ion or electron transfer mechanisms can then be probed and studied. For the transfer of a neutral species across such interface, however, it is not necessary to apply a potential difference. In a system in which initially the neutral species of interest is only present in one phase, i.e., the organic phase, partition of this species will take place across the boundary of the two liquids. Then, the concentration gradient established between the interface and the bulk of the second phase, i.e., an aqueous solution, will be the dominant driving force to move this species into it. This spontaneous transfer, along with diffusion into the bulk of the aqueous solution, should serve the purpose of delivering a neutral species to a substrate in the SECM experiments.

In line with the purpose mentioned above, a new micropipet delivery–substrate collection (MD–SC) mode of the SECM is proposed, and the representative operation scheme is shown in Figure 1. A micropipet with an ITIES is employed as the SECM tip to deliver the species of interest to the substrate, where the electrochemical reaction takes place. The micropipet is loaded with a water-immiscible organic solution containing the species of interest, R , that is soluble in both phases. Outside the micropipet an aqueous electrolyte is employed. Since the organic solvent is immiscible with the aqueous solution, only R will diffuse from the inside of the micropipet across the ITIES to the outside aqueous electrolyte. The micropipet, while delivering the species, is scanned parallel to the substrate, i.e., an electrocatalyst array or an electrode. R will diffuse into the aqueous solution and reach the substrate where, provided a suitable potential is applied, it will ultimately react to yield the spatial current response characteristic of a SECM image in the TG–SC mode.

We herein demonstrate the use of the MD–SC mode of the SECM. We chose two electrochemically reversible systems, namely the oxidation of ferrocenemethanol (FcMeOH) and the reduction of benzoquinone (BQ), and two electrocatalytic systems, the methanol and formic acid oxidation reactions (MOR and FAOR, respectively). Two-dimensional current response profiles of these electrochemical reactions carried out at a microscale

substrate or electrocatalytic reactions carried out on electrocatalyst arrays can be acquired as high-resolution SECM images. Digital simulations were also performed to understand the model system quantitatively.

EXPERIMENTAL SECTION

General. Ferrocenemethanol 97% (Aldrich, St. Louis, MO), 1,4-benzoquinone 98% (Aldrich, Milwaukee, WI), 1,2-dichloroethane 99+% (DCE, Fisher Scientific, Fair Lawn, NJ), acetonitrile 99.9+% (Aldrich, Milwaukee, WI), octyltriethoxysilane 96+% (Aldrich, Milwaukee, WI), formic acid 97% (Acros, NJ), sulfuric acid 94–98% (trace metal, Fisher Scientific, Canada), bis(triphenylphosphoranylidene)ammonium chloride 97% (BTPPA⁺Cl⁻, Aldrich, Milwaukee, WI), potassium tetrakis(4-chlorophenyl)borate 98+% (K⁺TPBCl⁻, Aldrich, Milwaukee, WI), glycerol 99.8% (Fisher Scientific, Fair Lawn, NJ), H₂PtCl₆·6H₂O 99.9% (Alfa Aesar, Ward Hill, MA), Ce(NO₃)₃·6H₂O 98.5+% (EM Science, Cherry Hill, NJ), Pb(NO₃)₂ (Fisher Scientific, Fair Lawn, NJ), sodium chloride (Fisher Scientific, Fair Lawn, NJ), Nafion perfluorinated resin solution 5 wt % in lower aliphatic alcohols and water (Aldrich, St. Louis, MO) were used as received. Glassy carbon (GC) plates (Alfa Aesar, Ward Hill, MA, 1 mm thick) were cut into 16 mm × 16 mm squares prior to use. All aqueous solutions were prepared using Milli-Q water (Millipore Co., Bedford, MA). A CHI Model 900B SECM (CH Instruments, Inc., Austin, TX) was employed to perform electrochemical experiments. The micropipets were prepared using a laser-based micropipet puller (model P-2000, Sutter Instrument Co., Novato, CA). A picoliter solution dispenser (CHI mode 1550, Austin, TX) was used to prepare electrocatalyst arrays.

Micropipet (Tip) Preparation. The micropipets were pulled from borosilicate capillaries (o.d./i.d. = 1.0/0.58 mm). Micropipets with opening diameters between 20 and 30 μm were fabricated, and the exact opening sizes were checked using an optical microscope before each experiment. To reduce the possibility of water penetration from the outside aqueous electrolyte into the micropipet, the inner wall of the micropipet was silanized by contact with octyltriethoxysilane overnight and then dried overnight to make it hydrophobic.^{12,14} The octyltriethoxysilane was injected into the micropipet from the back side and was blown out using an air stream, and the micropipet was allowed to dry overnight. For the delivery of FcMeOH or BQ, organic solutions of the corresponding compound were filled into the micropipet from the back side using a 10 μL syringe. For the delivery of MeOH or FA, a DCE solution containing 6 mM of BTPPA⁺TPBCl⁻ with the desired amount of MeOH or FA was filled into a micropipet, and a Ag wire (diameter = 100 μm) coated with Ag⁺TPBCl⁻ film was then inserted into the micropipet from the back side. The Ag⁺TPBCl⁻ coating on the Ag wire was prepared by electrodeposition from a 10 mM K⁺TPBCl⁻ aqueous solution using a potential of 1.0 V (vs Ag/AgCl) for 30 s.

Synthesis of BTPPA⁺TPBCl⁻. The BTPPA⁺TPBCl⁻ was prepared by the metathesis method.¹⁶ Equimolar amounts of BTPPA⁺Cl⁻ and Na⁺TPBCl⁻ were added into a solvent mixture of MeOH and water (3/1, v/v) to prepare a nearly saturated

(15) Zhan, D.; Li, X.; Zhan, W.; Fan, F.-R. F.; Bard, A. J. *Anal. Chem.* **2007**, *79*, 5225.

(16) Lee, H. J.; Beriet, C.; Girault, H. H. *J. Electroanal. Chem.* **1998**, *453*, 211.

solution. A foamlike white precipitate was formed and filtered out, thoroughly washed with water, and then dried under air. The resulting white powder was recrystallized twice using acetone, and slightly yellowish crystallites of $\text{BTPPA}^+\text{TPBCl}^-$ were obtained.

Pt Microelectrode (Substrate) Preparation. The Pt microelectrode (diameter = $100\ \mu\text{m}$) and the Au UME (diameter = $25\ \mu\text{m}$) were fabricated by heat-sealing the corresponding metal wire under vacuum in a borosilicate glass capillary.¹⁰ The bottom cross-section of the glass capillary was removed with sandpaper to reveal the metal disk, and the metal surface was then polished sequentially with alumina powder (from 1.0 to 0.3 to $0.05\ \mu\text{m}$). Cyclic voltammetry in 0.5 M sulfuric acid was employed to clean the Pt microelectrode and the Au UME surface before SECM experiments.

Preparation of Electrocatalyst Arrays. The electrocatalyst arrays with a series of different metal composition ratio spots were prepared on GC substrates according to the procedures described previously.¹ Using the Pt–Ce array as an example, solutions with 0.3 M H_2PtCl_6 and 0.3 M $\text{Ce}(\text{NO}_3)_3$ in water/glycerol solutions (3/1, v/v) were used as the precursors for the preparation of Pt–Ce mixtures. These precursor solutions were deposited successively onto a GC substrate by a picoliter solution dispenser to form an array of spots containing different volume ratios of the precursors. The as-prepared array was dried overnight at $150\ ^\circ\text{C}$ under Ar flow and then reduced under H_2 flow at $350\ ^\circ\text{C}$ for 1 h in a tube furnace. The average diameters of the spots thus prepared were about $250\ \mu\text{m}$. For the preparation of a Pt–Pb array, 0.3 M H_2PtCl_6 and 0.3 M $\text{Pb}(\text{NO}_3)_2$ in a water/glycerol solution was used as the precursor.

Reversible Hydrogen Electrode (RHE). A homemade RHE was used as the reference electrode for FAOR and MOR experiments. A negative potential ($-3.0\ \text{V}$ vs Ag/AgCl) was applied to a Pt wire (0.5 mm diameter) in a glass tube with a frit at its terminal to generate hydrogen bubbles. The glass tube was filled with 0.5 M sulfuric acid solution, and the generated hydrogen bubbles were maintained in contact with the Pt wire. The potential of the RHE was checked with respect to a commercial Ag/AgCl reference electrode after every preparation and was stable during the entire experimental time period.

SECM Imaging Experiments for FcMeOH Oxidation, BQ Reduction, and Electrocatalytic FAOR. A micropipet loaded with an organic solution of the species of interest was used as the tip in SECM imaging experiments. The substrate was a Pt microelectrode to which a suitable potential was applied, in this case $0.5\ \text{V}$ vs Ag/AgCl for FcMeOH oxidation and $-0.1\ \text{V}$ vs Ag/AgCl for BQ reduction. The plane parallel to the substrate surface is defined as the X – Y plane, and the Z direction is normal to the substrate surface with the surface point defined as $Z = 0$. The micropipet was scanned in the X and Y directions above the substrate, and the center of the substrate was found by locating the maximum current responses in both X and Y directional scans. The micropipet was positioned above the center of the substrate, and the tip–substrate distance was estimated by the substrate current response when the micropipet approached the substrate at a speed of $2\ \mu\text{m}\ \text{s}^{-1}$. At the end of the imaging process, the micropipet was crashed to the substrate to determine the $Z = 0$ point where a clear disturbance of the substrate current was

observed. A more accurate determination of the distance is detailed for the study of the MOR. A Ag/AgCl reference electrode was used for FcMeOH and BQ experiments, and for all experiments, the counter electrode was a gold wire. Solutions of NaSO_4 , NaCl , or H_2SO_4 were used as aqueous electrolyte and specified in their respective sections.

SECM Imaging Experiment for MOR on Electrocatalyst Arrays. The MD–SC mode SECM imaging of MOR on an electrocatalyst array consisted of three sequential procedures: (i) removal of any substrate tilt, (ii) determination of the micropipet tip–array substrate distance, and (iii) SECM imaging process. First, the tilt of the substrate was removed by running negative approach curves. The reference electrode was a RHE, and a Au wire was the counter electrode; the electrolyte was 0.5 M H_2SO_4 aqueous solution, and the tip carried out the oxygen reduction reaction (which provides negative feedback upon approach to GC at open circuit). The Au UME tip approached at three different locations surrounding the electrocatalyst array on the substrate as to form a triangle. The distance between each location (vertex of the triangle) was greater than $4000\ \mu\text{m}$. The substrate tilt was considered to be flat if the height differences in the Z direction (determined by negative approach curves) between these locations were smaller than $1\ \mu\text{m}$ per $1000\ \mu\text{m}$. For the determination of the tip–substrate distance, an ion transfer process across the ITIES was used. The Au UME tip was replaced by a micropipet tip which was loaded with MeOH in DCE solution containing 6 mM $\text{BTPPA}^+\text{TPBCl}^-$ and with a $\text{Ag}^+\text{TPBCl}^-$ coated Ag wire inserted in it. The electrolyte was replaced by 0.1 M Na_2SO_4 aqueous solution containing 2.5 mM TPrA^+Cl^- . A potential of 0 V (vs RHE) was applied to the Ag wire while the micropipet tip was approached toward the substrate, and the negative approach curve, thus, acquired was employed to determine the tip–substrate distance. Finally, for the imaging process, the Ag wire was removed from the micropipet tip and the electrolyte was changed to an Ar purged 0.5 M H_2SO_4 aqueous solution. An Ar blanket was kept above the electrolyte throughout the imaging processes. The micropipet tip was positioned at a desired distance above the substrate and then scanned in the X – Y plane. The substrate current response of each electrocatalyst spot was recorded, and a SECM image was, thus, obtained. Cyclic voltammetry experiments were performed between every imaging experiment to restore the surface condition of the electrocatalyst spots. The SECM scan rate was selected to be sufficiently slow so that the obtained images were relatively independent of tip scan rate.

Preparation of Carbon-Supported $\text{Pt}_{80}\text{Ce}_{20}$ Electrocatalyst. The preparation of 60 wt % Pt– CeO_2 electrocatalyst supported on Vulcan XC-72R is described. $\text{H}_2\text{PtCl}_6 \cdot 6\text{H}_2\text{O}$ (270 mg) and $\text{Ce}(\text{NO}_3)_3 \cdot 6\text{H}_2\text{O}$ (57 mg) were dissolved in a solvent mixture of deionized water (100 mL) and ethanol (30 mL), and Vulcan XC-72R (80 mg) was added into it. The mixture was sonicated for 30 min and then adjusted to pH = 10 by adding 1 M sodium hydroxide solution under vigorous stirring with a magnetic stir bar. NaBH_4 solution (5 wt % in deionized water, 20 mL) was then added into the mixture, and the mixture was continuously stirred for 2 h at room temperature to complete the reduction reactions. The mixture was allowed to stand

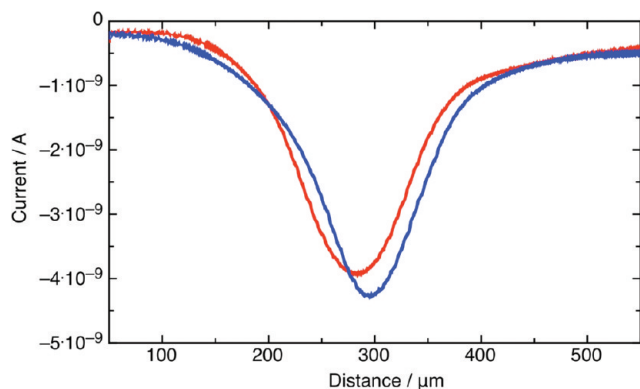


Figure 2. Substrate current responses of the MD–SC mode of the SECM when the micropipet tip was scanned in *X* (red) or *Y* (blue) directions above the substrate. The tip was a micropipet (opening diameter = 25 μm) and the substrate is a Pt microelectrode (diameter = 100 μm). The micropipet was loaded with 0.1 M FcMeOH in DCE, and the aqueous electrolyte outside the micropipet was 0.1 M NaCl. A constant potential of 0.5 V (vs Ag/AgCl) was applied to the substrate. The tip scan rate was 5 $\mu\text{m s}^{-1}$, and the tip–substrate distance was 30 μm .

overnight to precipitate the carbon-supported electrocatalysts. The precipitate was filtered and washed thoroughly with ethanol and deionized water and then dried under Ar flow at 120 $^{\circ}\text{C}$ overnight.

Chronoamperometric Experiments for Carbon-Supported Electrocatalysts. Ten milligrams of carbon-supported electrocatalyst was added into a solution of 0.5 mL of H_2O and 0.5 mL of ethanol, and the mixture was sonicated for 10 min to obtain the electrocatalyst ink. This ink (34 μL) was then deposited dropwise 2 $\mu\text{L} \times 17$ times onto a GC electrode (3 mm diameter). The deposited ink was allowed to dry under air before every next ink deposition. After the required amount of ink was deposited and dried on the GC electrode, it was then covered by 2 μL of Nafion solution. The electrolyte was a 0.5 M sulfuric acid solution containing 0.5 M MeOH. A RHE was used as the reference electrode, and the counter electrode was a graphite rod. The chronoamperometric MOR current responses of the prepared electrode were recorded at 600 s.

RESULTS AND DISCUSSION

Imaging of Electrochemical Reactions. FcMeOH is a neutral electroactive compound with reversible electrochemical behavior; therefore, its electrochemical oxidation reaction was chosen as a probe to test the feasibility of the MD–SC mode of the SECM. A micropipet loaded with 0.1 M FcMeOH in DCE was used as the SECM tip, and the substrate was a Pt microelectrode. The FcMeOH was delivered from the organic phase inside the micropipet tip to the outside aqueous electrolyte by spontaneous interfacial transfer and diffusion while it was scanned in *X* or *Y* directions at a close distance above a Pt microelectrode substrate. A potential of 0.5 V (vs Ag/AgCl) was applied at the Pt substrate to carry out the FcMeOH oxidation (experimental $E_{1/2} = 0.23$ V). As shown in Figure 2, reproducible anodic current responses were recorded at the Pt substrate when the micropipet tip was swept in either the *X* or *Y* direction. A distinct anodic current increase was observed as the tip scanned over the substrate and reached a maximum value when the tip passed by the substrate center. By finding the position of the maximum current responses in the *X*

and *Y* direction scan, the center of the Pt substrate can then be located. Once the center of the substrate has been found, approach curves of the micropipet moving toward the substrate can be acquired where the signal of interest is provided by the electrochemical collection of the transferring species by the substrate. The optimal approach speed was determined to be at less than 2.5 $\mu\text{m s}^{-1}$. Details concerning the effects of other approach speeds can be obtained in the Supporting Information, Figure S1.

Figure 3 shows the MD–SC mode SECM images of FcMeOH oxidation on a Pt microelectrode substrate. A micropipet loaded with FcMeOH in DCE was used to deliver FcMeOH to a Pt substrate, which is biased at a suitable potential to carry out the corresponding oxidation reaction. Figure 3 gives the distinct anodic substrate current response in terms of a high-resolution SECM image, which clearly indicates the location of the Pt surface and also depicts the corresponding reaction current profiles in close proximity to the substrate surface. Imaging of the BQ reduction on a Pt microelectrode substrate was also carried out and gave clear SECM images as well (see the Supporting Information, Figure S2). Accordingly, the MD–SC mode of the SECM is capable of imaging electrochemical reactions of neutral species on an electroactive substrate.

Digital Simulations. Digital simulations were performed to provide an estimate of the substrate current response due to the flux of FcMeOH from the inside of the micropipet to the outside electrolyte, as shown in Figure 4. The results of the simulation were compared to an experiment in which a micropipet loaded with FcMeOH in DCE was approached toward a Pt microelectrode substrate (100 μm diameter) at 1 $\mu\text{m s}^{-1}$, and the substrate FcMeOH oxidation current response was recorded (Figure 5).

2-D diffusion simulations with axial symmetry of the MD–SC system were carried out using the Comsol Multiphysics v.3.2 software (COMSOL, Inc., Burlington, MA). Details about the simulation setup can be found in the Supporting Information, where Figure S3 shows the geometry and boundary conditions of the problem. The analyte transfer at the ITIES was treated by defining two rate constants, k_f and k_b , which are shown schematically in Figure 4a as the outward and inward constants with respect to the micropipet. A partition coefficient, K , is defined as the ratio between these two constants (k_b/k_f) and can be regarded as an indicator of the affinity of electroactive species for the solvent inside the micropipet with respect to that of the aqueous phase. For FcMeOH, a $K \approx 150$ value is estimated by the ratio of the equilibrium concentrations in two solvent phases in a bulk experiment. In the micropipet system, however, such equilibrium assumption is only valid at the ITIES. Once the species is transferred across the ITIES, it is transported by diffusion into the bulk of the aqueous phase, where it is free to react at the substrate electrode. Figure 4b,c shows representative simulation results of a system with $K = 100$ and $K = 0.01$, respectively, with sufficiently large values of k_f and k_b so that the system is essentially at equilibrium. The system with $K = 100$ (high affinity for the organic phase) shows little exchange of material across the interface and no depletion of the species inside the micropipet. In contrast, the system with $K = 0.01$ (high affinity for the aqueous phase) shows enough

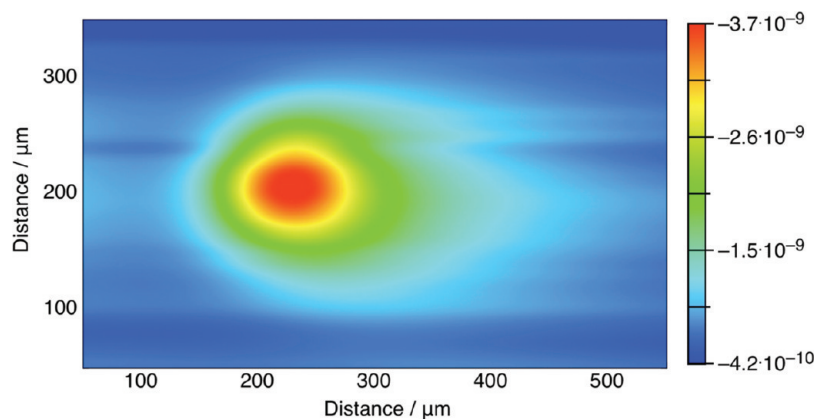


Figure 3. SECM image of FcMeOH oxidation at a Pt microelectrode. The micropipet was loaded with 0.1 M FcMeOH in DCE, and the opening diameter is 50 μm . The Pt microelectrode (diameter = 100 μm) was carrying out the FcMeOH oxidation at 0.5 V (vs Ag/AgCl). The micropipet scan rate was 50 $\mu\text{m s}^{-1}$, and the distance between the micropipet tip and the Pt substrate was 25 μm . The electrolyte was a 0.1 M NaCl aqueous solution. The scale bar shows current range in A.

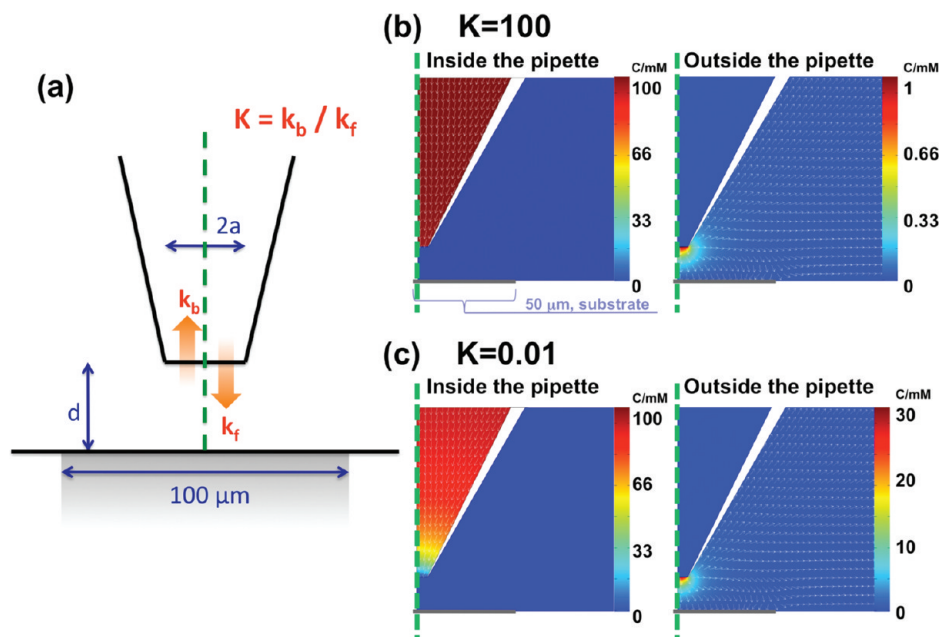


Figure 4. (a) Schematic representation of the transfer of FcMeOH across an organic/aqueous interface between the inside micropipet and the outside electrolyte. k_f and k_b are the forward and backward rate constants for the transfer of FcMeOH across the ITIES; d is the distance between the ITIES and the substrate, and a is the radius of the micropipet orifice. (b) and (c) are representative simulation results of a system with $K = k_b/k_f = 100$ and $K = 0.01$, respectively. Concentration profile snapshots are taken at $t = 200$ s and zoomed in to reveal an area of 100 $\mu\text{m} \times 100 \mu\text{m}$. Red arrows show the direction of the diffusive flux, and the green dashed line shows the axis of symmetry for the cylindrical geometry.

exchange of material across the interface to cause a large concentration gradient inside the micropipet.

Our simulation results indicate that the equilibrium assumption of the concentrations at the interface being related to the value of K is only valid when the values of k_b and k_f lead to diffusion control ($k > 0.01$ cm/s). Studies of ion transfer across ITIES have found values of the electrochemical standard transfer rate constants to be on the order of 0.01 to 0.1 cm/s,¹⁷ which indicate that such ion transfers are fast; therefore, we assume that this is the case for the transfer of a neutral species. Figure 5a shows the substrate responses for approach curves at different values of the parameter K when the values of k_b and k_f lead to no kinetic complications for a selected system, i.e., $k_b, k_f \gg 0.01$ cm/s. Notice that, as expected, larger values of K , which represent a higher affinity of the species to the organic phase

inside the micropipet, lead to smaller responses at the substrate. When lower values of K are evaluated, the response of the system tends to converge to a situation where the transport of species to the substrate is dominated by diffusion from the bulk of the micropipet to the outside.

Figure 5b shows the experimental result for the delivery of FcMeOH and its fit to the simulations. A minor correction must be applied to account for the difference in the diffusion coefficients of the species in the organic and aqueous environment; this was accounted for by the use of Walden's rule¹⁸ which relates the ratio of the diffusion coefficients in the phases to the ratio of the viscosities of the solvents. The fit is good throughout a reasonable

(17) Senda, M.; Kakiuchi, T.; Osakai, T. *Electrochim. Acta* **1991**, *36* (2), 253–262.

(18) Walden, P.; Ulich, H.; Busch, G. *Z. Phys. Chem.* **1926**, *123*, 429.

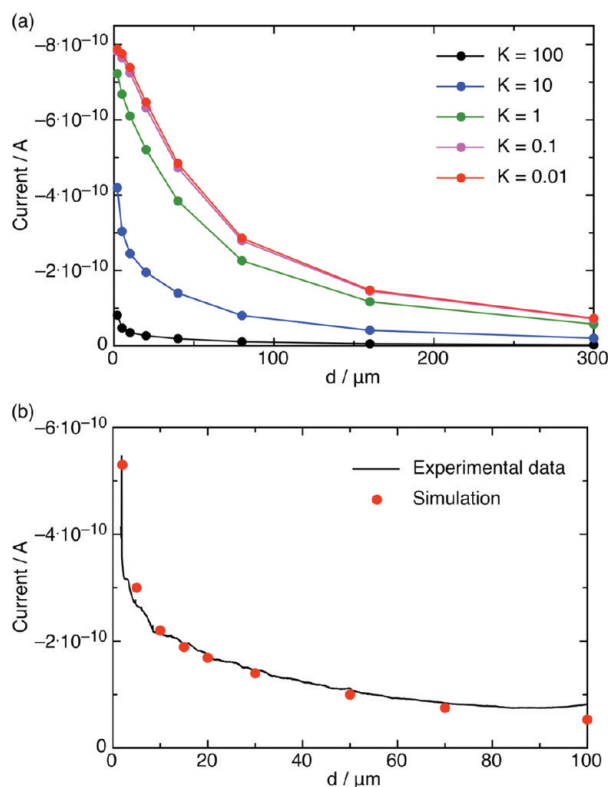


Figure 5. (a) Simulated substrate current responses when the micropipet tip is approached toward the substrate and having different values of K . The substrate diameter is $100 \mu\text{m}$, and the micropipet orifice diameter is $15 \mu\text{m}$. (b) Experimental and simulated ($K = 150$, $k_f = 100 \text{ cm/s}$, $k_b = 1.5 \times 10^4 \text{ cm/s}$) substrate FcMeOH oxidation current responses when a micropipet tip was approaching the substrate. The micropipet (opening diameter = $15 \mu\text{m}$) was loaded with 10 mM FcMeOH in DCE. The substrate was a Pt microelectrode (diameter = $100 \mu\text{m}$) at 0.5 V (vs Ag/AgCl). The approach speed was $1 \mu\text{m s}^{-1}$. The electrolyte was a 0.1 M NaCl aqueous solution.

distance range, which gives good confirmation of the proposed mechanism of delivery. Although FcMeOH is widely used as a mediator in aqueous environments, its solubility and affinity to DCE is larger than in water as evidenced by the value of $K \approx 150$. This case is similar to the one presented in Figure 4b, and it leads to substrate currents that are substantially lower than the maximum possible, as observed when comparing low and high values of K in Figure 5a. Thus, for analytes whose value of K does not favor their transfer, a natural answer is to increase their concentration in the organic phase. Doing so, however, may lead to other effects (e.g., dimerization, interfacial precipitation, perturbation of the ITIES) that should be taken into account for an accurate comparison of simulation and experiment. In the case of FcMeOH, we have observed that increasing its concentration in the DCE phase leads to fittings that are only satisfied by assuming smaller values of K in the simulation as shown in the Supporting Information, Figure S5.

Imaging of Electrocatalytic FAOR and MOR. With the success of imaging FcMeOH oxidation and BQ reduction reaction, we further extended the application of the MD–SC mode of the SECM to the imaging of electrocatalytic processes, such as the FAOR. Pt is known to be an electrocatalyst for FAOR,¹⁹ thus a Pt microelectrode was employed as the substrate. A micropipet

loaded with FA in DCE was employed to deliver the FA to the substrate. The electrocatalytic oxidation of FA is sluggish and of low efficiency; therefore a high concentration of FA was used to ensure larger current responses. The MD–SC mode SECM images of the FAOR at different substrate potentials are shown in Figure 6. The efficiency of FA oxidation at a Pt electrocatalyst is potential dependent. A more positive potential at the Pt substrate corresponds to a higher rate of the FAOR; thus, the anodic current response will be comparatively higher than the background current (possibly arising from the reduction of trace oxygen) and gives better resolution in the SECM image. As shown in Figure 6, clear and well-defined SECM images of FAOR on the Pt substrate can be acquired when the substrate potentials were 600 , 500 , and 400 mV (vs RHE). Although the FAOR image was somewhat blurred with background currents due to the lower FAOR rate when the applied potential was 300 mV (vs RHE), the location of the substrate was still evident through its distinguishable anodic current response.

The main motivation for this MD–SC mode of the SECM was to image MeOH oxidation in the MOR on different arrays with a series of electrocatalyst spots of different compositions. This serves as a high throughput screening method in the search for new multicomponent MOR electrocatalysts and their optimum compositions. The above-mentioned results demonstrate the ability of the MD–SC mode of the SECM in distinguishing different electrocatalytic activities of the substrate, which is the key requirement to employ the method for the electrocatalyst screening purpose.

For the SECM imaging of the MOR on an electrocatalyst array, the micropipet tip had to be scanned over a relatively larger area than in the previously presented cases. To obtain high quality SECM images without damaging the micropipet tip or the electrocatalyst spots during the imaging processes, precise control of the tip–substrate distance is crucial. The success in tip–substrate distance control by monitoring the substrate current responses during the tip-approaching process in the FcMeOH system described earlier is based mainly on the fact that the electrochemical redox behavior of FcMeOH is fast and highly reversible. The substrate can carry out the FcMeOH oxidation under diffusion controlled conditions and provide stable current responses. This added to the fact that the current recorded by a microelectrode shows much smaller background currents than those found with a GC array with a large number of catalyst spots.

The determination of the tip–substrate distance becomes different when the micropipet is used to deliver MeOH. The MOR is a sluggish and kinetically complicated reaction, where reaction intermediates, such as carbon monoxide or formates, can poison the electrocatalyst.^{20–23} It is, therefore, very difficult to obtain a stable substrate current response when a micropipet is delivering MeOH. Accordingly, the previously mentioned tip–substrate distance determination method for the FcMeOH system cannot be applied directly, and a new system with stable and position-dependent current responses is required.

(20) Cao, D.; Lu, G.-Q.; Wieckowski, A.; Wasileski, S. A.; Neurock, M. *J. Phys. Chem. B* **2005**, *109*, 11622.

(21) Housmans, T. H. M.; Wonders, A. H.; Koper, M. T. M. *J. Phys. Chem. B* **2006**, *110*, 10021.

(22) Iwasita, T. *Electrochim. Acta* **2002**, *47*, 3663.

(23) Wasmus, S.; Küver, A. *J. Electroanal. Chem.* **1999**, *461*, 14.

(19) Lu, G.-Q.; Crown, A.; Wieckowski, A. *J. Phys. Chem. B* **1999**, *103*, 9700.

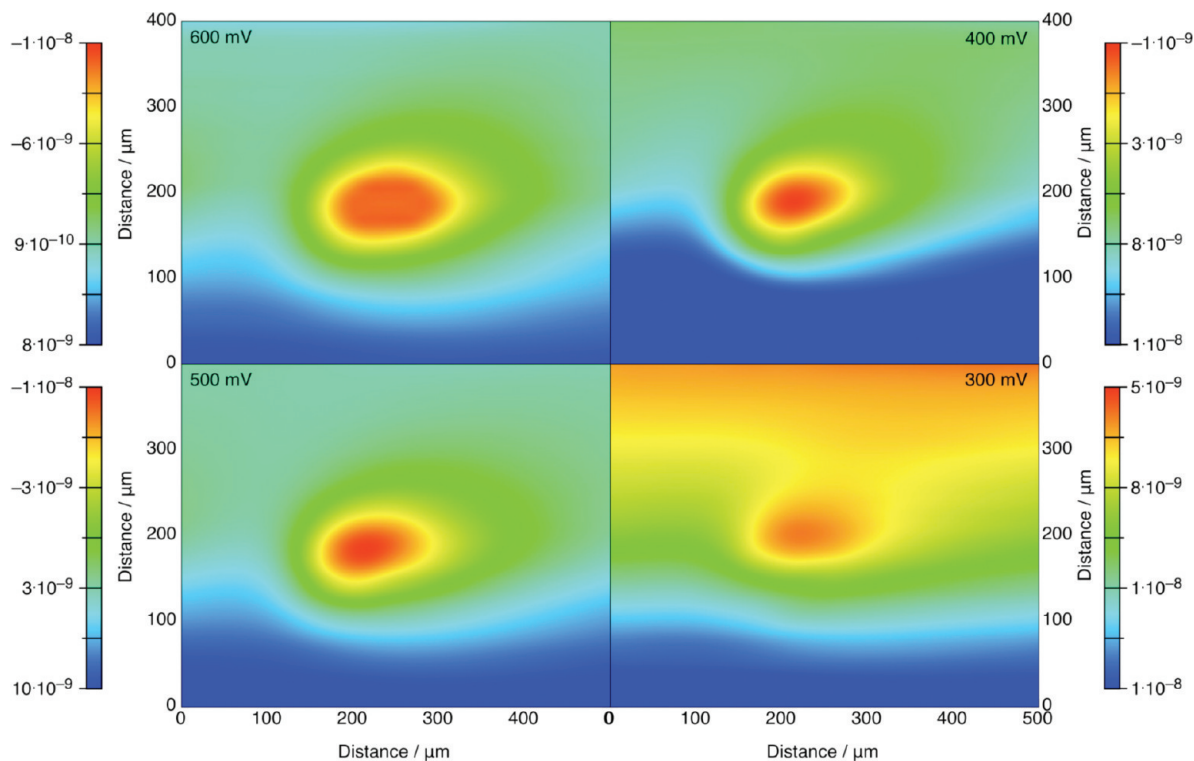


Figure 6. SECM images of FAOR on a Pt microelectrode at different applied potentials. The micropipet was loaded with 50% (v/v) FA in DCE, and the opening diameter was $15\ \mu\text{m}$. The Pt microelectrode (diameter = $100\ \mu\text{m}$) oxidized FA at potentials from 0.6 to 0.3 V (vs RHE). Five cycles of cyclic voltammetry experiments between 0.05 and 1.4 V (vs RHE) were carried out before every SECM image to clean the Pt microelectrode surface. The electrolyte was a 0.5 M sulfuric acid aqueous solution which was purged with Ar for 15 min before each experiment. The scan rate was $75\ \mu\text{m}\ \text{s}^{-1}$ ($15\ \mu\text{m}/0.2\ \text{s}$), and the tip–substrate distance was $20\ \mu\text{m}$. The tip–substrate distance was determined by crashing the micropipet after all SECM imaging processes. The scale bars show current range in A.

As mentioned in the introduction, the ion transfer properties across an ITIES under a potential bias have been studied with an ITIES suspended on a micropipet using the SECM. Such ion transfer phenomena provide position-dependent and stable current responses under diffusion-controlled conditions and was, therefore, employed to determine the tip–substrate distance in our system in parallel to MeOH flux. A micropipet tip was loaded with a mixture of DCE and MeOH and 6 mM BTPPA⁺TPBCl⁻, and the aqueous electrolyte outside the micropipet was 2.5 mM of tetrapropylammonium chloride (TPrA⁺Cl⁻) in 0.1 M NaSO₄. A silver wire coated with a Ag⁺TPBCl⁻ thin film was inserted into the micropipet organic phase and served as the working electrode, and the counter electrode was a gold wire in the aqueous electrolyte outside the micropipet. When a negative potential is applied between the working and the counter electrodes, the TPrA⁺ ion is transported from the aqueous phase to the organic phase inside the micropipet (see the Supporting Information, Figure S6). When the micropipet approaches the substrate, the flux of TPrA⁺ toward the micropipet is blocked, generating a negative feedback like response from which the distance to the substrate can be determined. Figure 7 shows a typical current–distance response (i.e., a negative feedback approach curve) of a micropipet tip approaching toward a GC substrate. Note the sudden current increase at the end of the tip-approach process recorded in Figure 7. The geometry of the ITIES can be altered by external applied pressures²⁴ or potentials.²⁵ Potential-dependent outward expansion of the interfacial meniscus during the ion transfer from an aqueous solution to the organic phase inside a micropipet was demonstrated in a

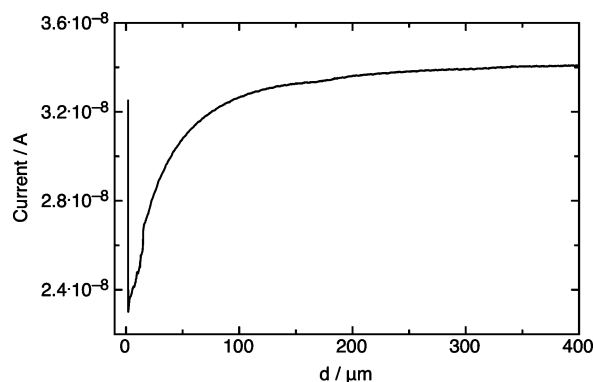


Figure 7. Typical current–distance curve of a micropipet tip with TPrA⁺ ion transfer across its ITIES during approach toward a GC substrate. The micropipet tip was loaded with 30% MeOH (volume ratio) in a DCE solution containing 6 mM BTPPA⁺TPBCl⁻. A Ag⁺TPBCl⁻ coated Ag wire was inserted in the micropipet and served as the working electrode. The RHE was used as the reference electrode, and the counter electrode was a Au wire. The electrolyte was 0.1 M Na₂SO₄ aqueous solution containing 2.5 mM TPrA⁺Cl⁻. The opening diameter of the micropipet was $25\ \mu\text{m}$, and its approaching speed toward the GC substrate was $2\ \mu\text{m}\ \text{s}^{-1}$. d is the distance between the meniscoid ITIES and the substrate.

previous study.²⁵ Solvents with very low solubility in the aqueous phase were used in these studies to ensure a minimum solvent exchange across the ITIES. However, when the micropipet tip was loaded with MeOH in an organic solvent, a meniscoid ITIES will be formed spontaneously as evidenced by direct observation

(24) Shao, Y.; Mirkin, M. V. *Anal. Chem.* **1998**, *70*, 3155.

under an optical microscope (see the Supporting Information, Figure S7). Such outward deformation of the ITIES could be due to the high affinity of MeOH toward the aqueous phase. In the negative feedback approach curves, the breakdown of the meniscoid ITIES as it touches the substrate caused an immediate increase of the inward TPrA⁺ flux, which resulted in the sudden current increase. The ITIES meniscus can rebuild itself as the micropipet is retracted from the surface, and reproducible negative approach curves could be acquired. For experimental purposes, the tip–substrate distance can, thus, be conveniently controlled by knowing where the ITIES meniscus touches the substrate. With the ability to accurately determine the tip–substrate distance when a micropipet is used to deliver MeOH, the MD–SC mode of the SECM is now ready to image the MOR at arrays with a series of different composition electrocatalyst spots.

The direct MeOH fuel cell (DMFC) is under investigation as a promising power source, converting the chemical energy of MeOH and O₂ into electricity by carrying out the MOR and ORR using electrocatalysts. However, the development of DMFC is hampered by the low efficiency and poor stability of the electrocatalysts available. Different screening methodologies have been developed for the purpose of fast searching of new electrocatalysts.^{1,26–28} Previously the TG–SC mode of the SECM has been demonstrated as a high-throughput method for finding new ORR electrocatalysts, and now, we use this new MD–SC mode of the SECM for the screening of MOR electrocatalysts.

Pt has high electrocatalytic activity toward MOR, but the intermediates generated during the process, such as carbon monoxide and formates, quickly poison it and, thus, shut down the MOR. Pt-based alloys or composites have been developed to circumvent such problems. PtRu is the most studied and representative electrocatalyst for the MOR, based on the general concept of generating hydroxyl radicals on the CO-free Ru that can oxidize the Pt bound CO and free up catalytic sites for MeOH dissociative adsorption. However, it still suffers from some instability because of dissolution of Ru during operation of DMFC, and it is also expensive. Recently, studies of the Pt–CeO₂ (Pt–Ce) systems reveal its potential in DMFC applications.^{29–37} Pt–Pb alloys have also shown better MOR electrocatalytic activities

compared to pure Pt electrocatalysts.^{38–40} Therefore, the MD–SC mode of the SECM was employed to image the MOR on Pt–Ce and Pt–Pb electrocatalyst arrays to demonstrate the feasibility of this method for MOR electrocatalyst screening.

A series of Pt–Ce and Pt–Pb electrocatalyst spots with different metal atomic ratios was prepared on a GC substrate by picoliter dispensing followed by a high-temperature hydrogen reduction treatment. The Pt–Ce spots prepared should be a composite of Pt and CeO₂, but the notation of Pt–Ce shows the atomic metal ratios of each spot. Figure 8 shows the SECM images of the MOR on these arrays with different applied potentials. The Pt₈₀Ce₂₀ and the Pt₆₀Pb₄₀ spots showed the highest MOR activities among all the spots in their corresponding arrays. MOR activity on the Pt₈₀Ce₂₀ spot can be observed at all three applied potentials, but no MOR activity on the Pt₆₀Pb₄₀ spot was seen when the applied potential was 600 mV. The Pt₈₀Ce₂₀ spot showed higher MOR activity than the Pt₆₀Pb₄₀ spot, as seen by comparing their maximum current responses. SECM images of MOR on a ternary Pt–Ce–Pb electrocatalyst array were also acquired (see the Supporting Information, Figure S8), and consistent results were obtained.

The electrocatalytic MOR or FAOR involves multistep reaction mechanisms, and their side products or intermediates can easily poison the electrocatalyst. Therefore, cyclic voltammetry experiments were performed between every SECM imaging processes to clean and restore the electrocatalyst surface to its initial condition, and then, reproducible results can be acquired during successive SECM imaging experiments.

Chronoamperometric Characterization. To demonstrate, as has been done earlier with ORR electrocatalysts, that those prepared by screening predict similar behavior in larger carbon-supported electrocatalyst studies, after the electrocatalyst optimum composition was acquired from the SECM imaging experiments, the Pt₈₀Ce₂₀ electrocatalyst was then synthesized on a carbon (Vulcan XC-72R) support, and its MOR activity was compared with the commercial Pt₅₀Ru₅₀/C (BASF, C13–60 60% HP Pt/Ru alloy (1:1 a/o) on Vulcan XC-72) electrocatalyst by larger scale chronoamperometric experiments. As shown in the Figure 9, the Pt₈₀Ce₂₀/C exhibited statistically similar MOR activities as the Pt₅₀Ru₅₀/C over the potential range tested. These results suggest the MD–SC mode of the SECM method is feasible for the screening of multicomponent MOR electrocatalysts and determining their optimum composition.

CONCLUSIONS

The MD–SC mode of the SECM imaging method is demonstrated. A micropipet tip loaded with an organic solution was used to deliver a neutral species of interest, such as FcMeOH, BQ, formic acid, or MeOH to a substrate in an aqueous electrolyte. Suitable potentials were applied to the substrate to carry out the corresponding electrochemical or electrocatalytic reactions. The spontaneous transfer of the analyte across the ITIES and its

- (25) Dale, S. E. C.; Unwin, P. R. *Electrochem. Commun.* **2008**, *10*, 723.
 (26) Reddington, E.; Sapienza, A.; Gurau, B.; Viswanathan, R.; Sarangapani, S.; Smotkin, E. S.; Mallouk, T. E. *Science* **1998**, *280*, 1735.
 (27) Strasser, P.; Fan, Q.; Devenney, M.; Weinberg, W. H.; Liu, P.; Nørskov, J. K. *J. Phys. Chem. B* **2003**, *107*, 11013.
 (28) Stevens, D. A.; Rouleau, J. M.; Mar, R. E.; Bonakdarpour, A.; Atanasoski, R. T.; Schmoekkel, A. K.; Debe, M. K.; Dahn, J. R. *J. Electrochem. Soc.* **2007**, *154*, B566.
 (29) Xu, C.; Shen, P. K. *Chem. Commun.* **2004**, 2238.
 (30) Tang, Z.; Lu, G. *J. Power Sources* **2006**, *162*, 1067.
 (31) Xu, C.; Zeng, R.; Shen, P. K.; Wei, Z. *Electrochim. Acta* **2005**, *51*, 1031.
 (32) Campos, C. L.; Roldan, C.; Aponte, M.; Ishikawa, Y.; Cabrera, C. R. *J. Electroanal. Chem.* **2005**, *581*, 206.
 (33) Takahashi, M.; Mori, T.; Ye, F.; Vinu, A.; Kobayashi, H.; Drennan, J. J. *Am. Ceram. Soc.* **2007**, *90*, 1291.
 (34) Wang, J.; Deng, X.; Xi, J.; Chen, L.; Zhu, W.; Qiu, X. *J. Power Sources* **2007**, *170*, 297.
 (35) Ahn, H.-J.; Jang, J.-S.; Sung, Y. E.; Seong, T.-Y. *J. Alloys Compd.* **2009**, *472*, L28.
 (36) Scibioh, M. A.; Kim, S.-K.; Cho, E. A.; Lim, T.-H.; Hong, S.-A.; Ha, H. Y. *Appl. Catal., B* **2008**, *84*, 773.
 (37) Zhao, J.; Chen, W.; Zheng, Y. *Mater. Chem. Phys.* **2009**, *113*, 591.

- (38) Casado-Rivera, E.; Volpe, D. J.; Alden, L.; Lind, C.; Downie, C.; Vázquez-Alvarez, T.; Angelo, A. C. D.; DiSalvo, F. J.; Abruña, H. D. *J. Am. Chem. Soc.* **2004**, *126*, 4043.
 (39) Maksimuk, S.; Yang, S.; Peng, Z.; Yang, H. *J. Am. Chem. Soc.* **2007**, *129*, 8684.
 (40) Papadimitriou, S.; Tegoua, A.; Pavlidou, E.; Kokkinidis, G.; Sotiropoulos, S. *Electrochim. Acta* **2007**, *52*, 6254.

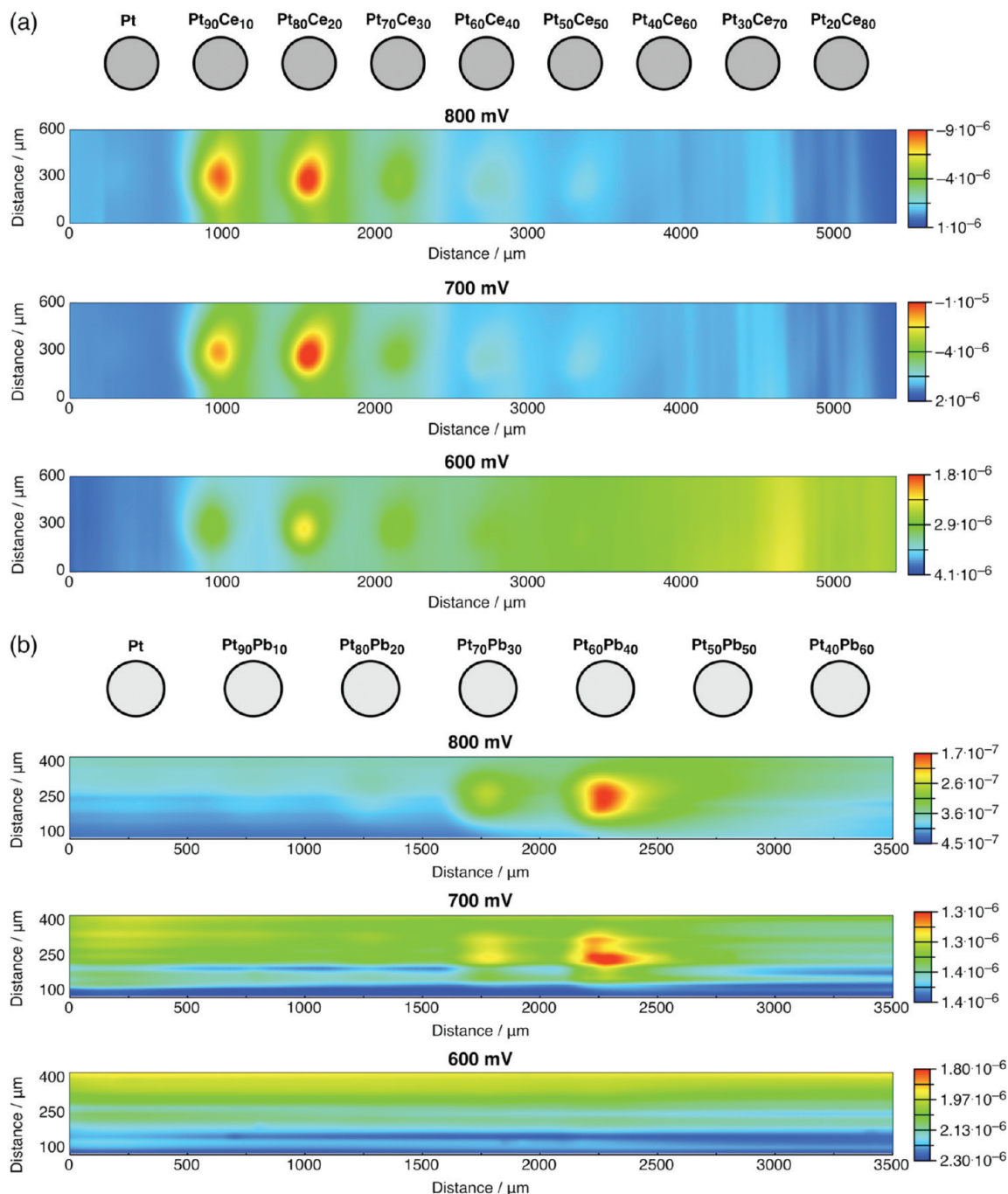


Figure 8. MD-SC mode SECM images of MOR on (a) a Pt-Ce array (the micropipet opening = $11 \mu\text{m}$) and (b) a Pt-Pb array (the micropipet opening = $15 \mu\text{m}$) under different applied potentials. The micropipet tip was loaded with DCE solution with 30% MeOH and 6 mM BTPPA⁺TPBCl⁻, and the tip-substrate distance was $30 \mu\text{m}$. A Au wire was used as the counter electrode, and the reference electrode was a RHE. The electrolyte was an Ar purged 0.5 M H₂SO₄ aqueous solution. The micropipet tip scan rate was $125 \mu\text{m s}^{-1}$ ($25 \mu\text{m}/0.2 \text{ s}$). The scale bars show current range in A.

diffusion toward the bulk of the aqueous solution served as the mechanism to deliver the neutral species to the substrate. The electrochemical or the electrocatalytic reactions at the substrate surface could be probed by scanning the tip parallel to the substrate in a close distance, and the two-dimensional current response profiles can be displayed as high-resolution SECM images. Digital simulations gave quantitative information of the tip-substrate distance and about the expected current response at the substrate.

Different electrocatalytic efficiencies for the FAOR on a Pt microelectrode can be readily distinguished by the MD-SC mode SECM images. High-resolution MD-SC mode SECM images of MOR on the Pt-Ce, Pt-Pb, and Pt-Ce-Pb electrocatalyst arrays under different applied potentials were acquired. The Pt₈₀Ce₂₀ and the Pt₆₀Pb₄₀ electrocatalysts showed superior MOR activities among all other spots in their corresponding arrays. The Pt₈₀Ce₂₀ spot shows higher MOR activity than Pt₆₀Pb₄₀ by comparing their anodic current responses on a Pt-Ce-Pb

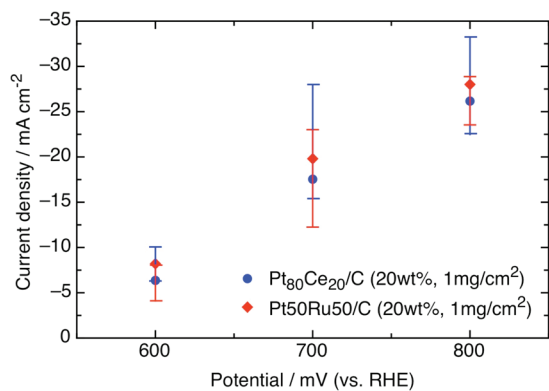


Figure 9. MOR activity of Pt₈₀Ce₂₀/C and Pt₅₀Ru₅₀/C under different applied potentials. The electrolyte was an Ar purged 0.5 M sulfuric acid solution containing 0.5 M MeOH, and a graphite rod was used as the counter electrode.

array. Carbon-supported Pt₈₀Ce₂₀ electrocatalyst was synthesized, and its MOR performance was comparable to the commercial Pt₅₀Ru₅₀/C electrocatalyst. These results suggest

the MD–SC mode of the SECM is feasible for the screening of multicomponent MOR electrocatalysts and determining their optimum composition for electrocatalytic reactions.

ACKNOWLEDGMENT

This work has been supported by MURI [DoD, Office of Naval Research (N00014-07-1-0758)], and the Robert A. Welch Foundation (F-0021). J.R.-L. thanks the Livingston Endowment for a research fellowship and Secretaría de Educación Pública of Mexico and the Mexican Government for complementary scholarship support.

SUPPORTING INFORMATION AVAILABLE

Additional information as noted in text. This material is available free of charge via the Internet at <http://pubs.acs.org>.

Received for review June 30, 2009. Accepted September 26, 2009.

AC901434A